Published online 15 July 2016

Nucleic Acids Research, 2016, Vol. 44, No. 15 ***7373–7384***
doi: 10.1093/nar/gkw634

Insight into G-quadruplex-hemin DNAzyme/RNAzyme: adjacent adenine as the intramolecular species for remarkable enhancement of enzymatic activity

Wang Li[1,†], Yong Li[1,†], Zhuoliang Liu[1], Bin Lin[2], Haibo Yi[1], Feng Xu[1], Zhou Nie[1,*] and Shouzhuo Yao[1]

[1]State Key Laboratory of Chemo/Biosensing and Chemometrics, College of Chemistry and Chemical Engineering, Hunan University, Changsha 410082, P. R. China and [2]Department of Medicinal Chemistry, School of Pharmaceutical Engineering & Key Laboratory of Structure-Based Drug Design & Discovery, Ministry of Education, Shenyang Pharmaceutical University, Shenyang 110016, P. R. China

Received February 1, 2016; Revised June 28, 2016; Accepted June 29, 2016

ABSTRACT

G-quadruplex (G4) with stacked G-tetrads structure is able to bind hemin (iron (III)-protoporphyrin IX) to form a unique type of DNAzyme/RNAzyme with peroxidase-mimicking activity, which has been widely employed in multidisciplinary fields. However, its further applications are hampered by its relatively weak activity compared with protein enzymes. Herein, we report a unique intramolecular enhancement effect of the adjacent adenine (EnEAA) at 3′ end of G4 core sequences that significantly improves the activity of G4 DNAzymes. Through detailed investigations of the EnEAA, the added 3′ adenine was proved to accelerate the compound I formation in catalytic cycle and thus improve the G4 DNAzyme activity. EnEAA was found to be highly dependent on the unprotonated state of the N1 of adenine, substantiating that adenine might function as a general acid–base catalyst. Further adenine analogs analysis supported that both N1 and exocyclic 6-amino groups in adenine played key role in the catalysis. Moreover, we proved that EnEAA was generally applicable for various parallel G-quadruplex structures and even G4 RNAzyme. Our studies implied that adenine might act analogously as the distal histidine in protein peroxidases, which shed light on the fundamental understanding and rational design of G4 DNAzyme/RNAzyme catalysts with enhanced functions.

INTRODUCTION

G-quadruplexes (G4) are non-canonical nucleic acid structures with stacked G-tetrads assembled by Hoogsteen hydrogen-bonding (1). Because of their unique structures and important biological functions, G4 have attracted intensive research interests. One of the most fascinating aspects of the G4 is that it can associate with hemin (iron (III)-protoporphyrin IX) to form peroxidase-mimicking G4 DNAzymes (and RNAzymes) (2). These DNAzymes/RNAzymes manifest the catalytic ability of nucleic acid in peroxidation reaction, one fundamental reaction type in aerobic metabolism, and thereby suggest a prototype of peroxidase in the prebiotic 'RNA world' hypothesis (3–5). In comparison with natural protein peroxidases, G4 DNAzymes/RNAzymes possess advantages of small size, easy synthesis, facile manipulation and amenability to rational design of allosteric control, presenting a powerful catalytic toolkit in biosensing, biomaterials and bio-molecular devices (6–8). G4 DNAzymes have been extensively exploited as the signal producer to develop various biosensors and molecular machines (9–15), and the promising bio-catalyst in both aqueous and non-aqueous media (16–18). Moreover, recent *in vitro* evidences have proved that the peroxidase activity of hemin can be enhanced by several G-rich sequences derived from genomic elements such as telomeres, gene promoters and RNA transcripts, suggesting the oxidative damage potential of putative heme/G4 complexes within cells (19,20). Therefore, investigation on the catalytic activity and mechanism of G4 DNAzyme/RNAzyme has great implications for multidisciplinary fields.

Despite the listed advantages, the bio-catalytic application of G4 peroxidase has been limited due to its much lower activity than that of protein peroxidases, such as the horseradish peroxidase (HRP). Therefore, continuous

*To whom correspondence should be addressed. Tel: +86 731 8882 1626; Fax: +86 731 8882 1848; Email: niezhou.hnu@gmail.com
†These authors contributed equally to the paper as first authors.

efforts have been made to improve the activity of G4 DNAzyme. *In vitro* selection using systematic evolution of ligands by exponential enrichment (SELEX) and the screening of known G4-forming sequences are two conventional approaches for developing nucleic acid peroxidases (3,19,21–23). As a result, a number of G4 sequences with potent activity have been discovered and the topological analysis on these G4 sequences indicates that parallel G4 structure is preferable for high peroxidase activity. Another popular strategy is the addition of exogenous activity-boosting agents, such as nitrogenous buffers (2), adenosine triphosphate (24,25), DOTASQ (26,27) and spermine (28). This strategy is intriguingly useful, but its implementation usually requires high concentration of the boosting agents because of the intermolecular enhancing effect. The most recently reported method is to enhance the activity of the G4 DNAzyme by flanking d(CCC) sequence (29). The enhancement effect, however, is still relatively moderate (∼ 3-fold) and there is a deficiency of thorough research into the mechanism of the enhancement. Thus, it continues to be desirable yet challenging to develop a facile and versatile approach to efficiently improve G4 DNAzyme activity.

After millions of years of molecular evolution, natural protein peroxidases, e.g. HRP, obtain a delicate pocket accommodating hemin to greatly facilitate the hemin-mediated peroxidation reaction (30). In the hemin pocket, the axial proximal histidine covalently coordinates with the ferric ion of hemin, while another key histidine at the distal site plays a crucial role as a general acid–base catalyst that significantly accelerates the peroxidation reaction (31). Correspondingly, in G4 DNAzymes/RNAzymes, it is speculated that guanines in G-tetrad might serve as the proximal ligand comparable to the proximal histidine in HRP (24,32). However, it is generally believed that G4 DNAzymes appear to lack the distal ligand that functions as the general acid–base catalyst (33), leading to their low activity. Hence, the following question is raised: can nucleobase, resembling the histidine in HRP, function as the distal ligand of hemin for the general acid–base catalysis in the DNA/RNA-catalytic peroxidation? The answer to this question will shed much light on the fundamental understanding of G4 peroxidases catalysis and provide the guidance on the rational modification of these enzymes.

Herein, we report a unique intramolecular enhancement effect of the proximal adenine for the peroxidase activity of a G4 DNAzyme, termed enhancement effect of adjacent adenine (EnEAA). Our detailed investigation provides a deep insight into the mechanism of EnEAA, in which the adenine base presumably acts as the distal species for the general acid–base catalysis in DNA/RNA-catalytic peroxidation. The pivotal active groups of adenine to participate in the catalysis have been identified. We have proved that the EnEAA is applicable for a variety of reductive substrates, buffer conditions, G4 DNAzymes with parallel structures and even G4 RNAzyme, presenting a general strategy to enhance the nucleic acid peroxidase activity. These findings contribute insightful information to the further understanding of the catalytic mechanism of G4 DNAzyme/RNAzyme, the rational design of advanced nucleic acid peroxidases and the primordial peroxidation catalysis in 'RNA world' hypothesis.

MATERIALS AND METHODS

Materials and reagents

Tris(hydroxymethyl)aminomethane (Tris), 4-(2-hydroxyethyl)-1-piperazineethanesulfonic acid (HEPES), 2-(4-Morpholino)ethanesulfonic acid (MES), 2,2′-azinobis(3-ethylbenzothiozoline-6- sulfonic acid) diammonium salt ($ABTS^{2-}$), 3,3′,5,5′-tetramethylbenzidine (TMB), amplex red (AR), luminol and the DEPC-treated water were obtained from Sangon Biotech (Shanghai, China). Triton X-100, H_2O_2 of 30% v/v, citric acid, hemin, dimethylsulfoxide (DMSO) were purchased from Sigma-Aldrich. Hemin was dissolved in DMSO and diluted to 10 mM, then stored in the dark place at 4°C for further experiment. Freshly prepared H_2O_2 was done on the spot by directly diluting the high concentration H_2O_2 of 30% v/v (∼10 M) to the desired concentration (10 mM) for use. All the buffers were prepared from the ultrapure water (18.25 MΩ·cm, 25°C) purified by a Millipore filtration system, and were filtered through 0.22 mm cellulose acetate membranes and stored at 4°C in refrigerator before use. The inorganic salts and the other organic chemicals employed here were highest quality of analytical grade.

The DNA and RNA oligonucleotides used in this work were purchased from Sangon Biotech and Takara (Dalian, China) respectively, while purine derivative modified DNA oligonucleotides were synthesized by TriLink (San Diego, CA, USA), of which all the complete sequences are listed in Supplementary Tables S1 and 2. All DNA or RNA samples were dissolved in ultrapure water at room temperature and were quantified by $OD_{260\,nm}$ using the molar extinction coefficient value provided by the manufacturers. To prepare DNA G4 or perform DNA hybridization, the DNA oligos were annealed by heating to 95°C for 5 min, cooling in ice for 2 h to favor the oligonucleotides folding and then were stored at 4°C. Similar process was conducted to prepare RNA G4 except the initial step heating to 70°C for 5 min.

G4 DNAzyme-catalyzed peroxidation

The UV-vis spectra of the DNAzyme peroxidation product of $ABTS^{\bullet-}$ were collected on BECKMAN DU-800 spectrophotometer. The annealed G-quadraplex DNAs (100 nM) diluted from the corresponding stock solutions were incubated with hemin (100 nM) in MES buffer (25 mM MES, 200 mM NaCl, 10 mM KCl, 1% DMSO, 0.05% Triton X-100, pH 5.1) for 0.5 h at 25°C. After the formation of DNA–hemin complexes, the solution was transferred to 1 mm quartz cuvette, following the addition of $ABTS^{2-}$ (2 mM) and H_2O_2 (2 mM) and then incubated in the UV-vis cuvette at 25°C for 2 min after which the UV-vis spectrum was collected in the range of 400–800 nm at a speed of 1200 nm/min. The same samples were prepared to take photographs under the digital camera (Canon EOS70D).

The catalytic kinetics experiments were performed on DU-800 using the Kinetics/Time mode. The G-quadraplex DNAs (100 nM) were incubated with hemin (100 nM) in MES buffer in the 1 mm quartz cuvette placed at UV-vis cuvette holder for 0.5 h at 25°C. Then, upon $ABTS^{2-}$ (2 mM) and H_2O_2 (2 mM) added, reactions were initiated and

kinetics were followed by monitoring the appearance of the radical anion (ABTS•⁻) at 415 nm for 120 s. The concentration of ABTS•⁻ was calculated based on the extinction coefficient of ABTS•⁻ (36 000 M^{-1}•cm^{-1}). Increases in the concentration of ABTS•⁻ were formulated as a function of time. In addition, the reaction rates (V_{DNA}) were obtained by calculating the slope of the linear portion of increases of concentration of ABTS•⁻ versus time.

Quantum mechanical calculation of the interaction between adenine derivatives and H_2O_2

All structures of complexes were optimized using density function theory (DFT) calculations (Becke three parameters with the Lee-Yang-Parr functional (B3LYP)) and Møller Plesset second-order perturbation theory (MP2). In the geometry optimization and thermodynamic properties, the aug-cc-pVDZ basis set was used. The basis set superposition error correction was taken into account. All calculations in this work were carried out using a suite of Gaussian 09 programs.

Please see supporting information (SI) for the experimental details of pH dependence and buffer dependence of G4 DNAzyme activity, acid-alkaline transition of resting G4 DNAzyme, spectroscopic characterization of peroxidation intermediate, fluorescent measurement of FAM-tagged G4–hemin complexes, circular dichroism (CD) measurements, molecular docking and molecular dynamics simulations and the determination of dissociation constants (K_d) of G4–hemin complexes.

RESULTS

Enhancement of G4 DNAzyme activity by 3′ adjacent adenine

To evaluate the influence of adjacent nucleobase on G4 DNAzyme activity, the most widely-used G4 DNAzyme sequence, namely Dz-00 here, was selected as the prototypical DNAzyme and different nucleotides were added on the each ends (3′ or 5′) of Dz-00 (Supplementary Table S1). The DNAzyme activity was probed by measuring the initial rate (V_0) of the oxidation of $ABTS^{2-}$ to a green colored ABTS•⁻ by H_2O_2. The reaction was carried out in MES buffer with 10 mM KCl at pH 5.1, since it was found the nitrogenous buffer and K^+ ion were favorable for high activity of G4 DNAzymes (3), and a linear kinetic profile could be obtained because ABTS•⁻ was stable in weakly acid medium (34). Interestingly, there is a 5.1-fold increase of V_0 value in G4 DNAzyme with added-3′A (Dz-11) compared with the Dz-00, revealing a significant improvement of the DNAzyme activity (Figure 1). In contrast, the influence of other variants on the DNAzyme activity is negligible. Given the adenine-specificity and 3′ end-selectivity of this nucleobase-caused activity enhancement, we hereby named it as the EnEAA.

Folding topology, structural stability and hemin binding of Dz-00 and Dz-11

To understand the mechanism of EnEAA, we first investigated different influential factors considering the interaction between the activity of G4 DNAzyme and the topology, thermal stability and hemin-binding affinity of G4. Both Dz-00 and its 3′A-variant Dz-11 show identical CD spectra with a strong positive signal at 263 nm and a negative signal at 243 nm (Supplementary Figure S1) (19), indicating that they are same parallel G4 conformers. The almost indistinguishable denaturation curves and the resulting Tm of Dz-00 and Dz-11 in the thermal melting CD experiments suggest their similar thermal stability (Supplementary Figure S2). Therefore, the structural alternation of G4 is excluded from the mechanism of EnEAA. Close similarity of hydrophobic pockets for docking hemin between Dz-00 and Dz-11 is evident that both exhibit intense Soret bands of hemin at 404 nm with extinction coefficients of more than 1.4 × 10^5 M^{-1} cm^{-1} (Supplementary Figure S3 and Table 1). The observation of the E band (501 nm) and D band (629 nm) of hemin in both complexes (Table 1) reveals that both DNAzymes contain the same high-spin hexa-coordinate ferric center (3). The nearly identical titration curves of Soret absorption band of hemin in response to Dz-00 and Dz-11 imply that these sequences bind hemin with similar affinity (Supplementary Figure S4). Further Job plot (Supplementary Figure S5A) and Scatchard analysis (Supplementary Figure S5B and C) indicate that the binding stoichiometry of hemin/DNA is 1:1 for both Dz-00 and Dz-11, consistent with the stoichiometry found

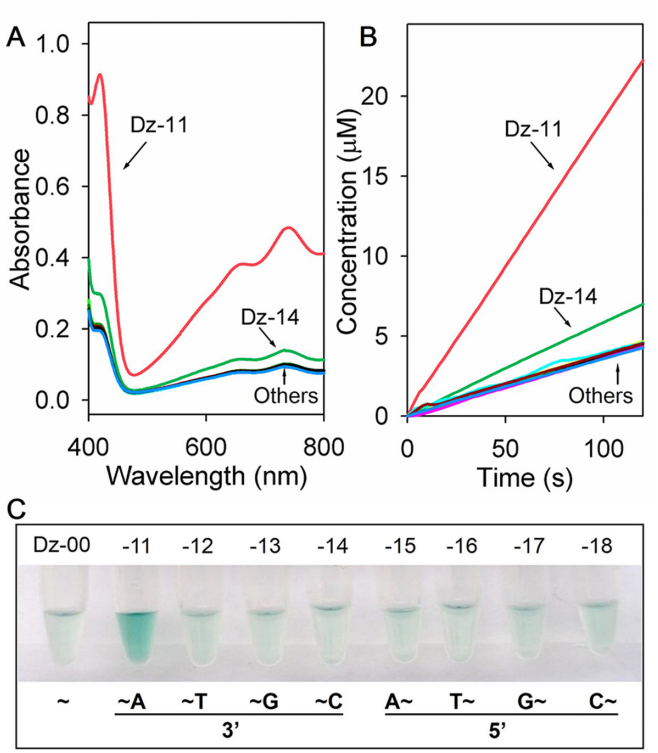

Figure 1. Effect of different adjacent nucleobases on G4 DNAzyme activity. (**A**–**C**) Represent the absorption spectra, the dynamic change of the concentration and the photographs of the peroxidation product (ABTS•–), respectively. The symbol '~' represents the sequence of Dz-00 (5′-GGGTAGGGCGGGTTGGG-3′). For other DNAzyme variants, one of four nucleotide bases (A, T, G or C) is added at 3′ (Dz-11 to -14) or 5′ end of Dz-00 (Dz-15 to -18), respectively.

in other G4 DNAzymes (2,26,35) and the calculated dissociation constant (K_d) of Dz-00-hemin (36 ± 2 nM) is almost the same as that of Dz-11-hemin (30 ± 3 nM). The unchanged hemin-binding affinity, in combination with the electronic absorption spectra of Dz-11 and Dz-00, indicates that the additional 3′A does not directly participate in the binding of hemin. Altogether, the similarity of the topology, thermal stability and hemin-binding affinity of G4 between Dz-11 and Dz-00 has been confirmed by all the above-mentioned characterizations, which can't be applied to explain the EnEAA properly. Thus, further studies on the mechanism of EnEAA should go beyond the conventional consideration of activity-influential factors.

Activity analysis of structural variants of G4 DNAzymes

In order to further investigate EnEAA, a number of different structural variants of G4 DNAzymes were designed and examined. To begin with, the understanding of binding mode of hemin with G4 DNAzyme is prerequisite for rational sequence design of DNAzyme variants. The end-capping mode of the porphyrin molecules binding to the G4 through strong π–π interaction has been substantiated by previously reported crystal structures and nuclear magnetic resonance (NMR) evidences (36,37). As our results have confirmed that both Dz-11 and Dz-00 adopt parallel G4 topology and the stoichiometric ratio of hemin:G4 of 1:1, it lead us to the question whether 3′ end- or 5′ end-G-tetrad is more preferable for hemin stacking (shown in Figure 2A). To answer this question, the fluorescent quenching experiments were performed using FAM-tagged DNA probes to monitor hemin-stacking because of the quenching ability of hemin to proximate fluorophore via electron transfer (38,39). As shown in Supplementary Figure S6, the fluorescence of 3′-FAM-Dz-00 is quenched substantially by hemin binding, while that of 5′-FAM-Dz-00 is only slightly affected, thereby indicating the preference of hemin stacking on 3′-G-tetrad. This result is consistent with the observed 3′ end specificity of EnEAA, further implying the proximity of 3′A to hemin.

To evaluate the proximity effect of 3′A on EnEAA we designed the first set of G4 variants with poly-T spacer (Tn, n = 0–8) upstream of 3′A (Figure 2B). Compared to the maximal activity (11.7 μM/min) of the Dz-11 ($n = 0$), insertion of one T spacer decreases enzymatic activity to 7.8 μM/min and further elongation of T spacer ($n \geq 2$) totally eliminates the A-induced activity enhancement, clearly proving that EnEAA is a short-range interaction. Next, the possibility of multiplying activity enhancement by poly-A at 3′ end (An, $n = 0$–16) was also probed. As shown in Figure 2C, the addition of more A ($n \geq 2$) does not lead to further improvement of the DNAzyme activity, verifying the predominant contribution of the first A adjacent to G4 to EnEAA.

Furthermore, the effect of the 3′A orientation on DNAzyme activity was investigated. One of G4 DNAzyme variants (Dz-41) with an intramolecular duplex structure was designed to confine 3′A pointing away from 3′-G-tetrad. Its activity decreases sharply to only about 0.3-fold of Dz-11 (Figure 2D), while its Soret band is unchanged relative to that of Dz-11 (Supplementary Figure S7), indicating the activity decrease is not due to the change of DNA-hemin binding. This result evinces that the orientation of A relative to the 3′-G-tetrad is also of significance for EnEAA. In another designed DNAzyme variant, we placed the A contiguous to 3′-G-tetrad by using an intermolecular duplex (Dz-61a:c, Figure 2E). A 3-fold increase of V_0 value in Dz-61a:c as compared with the Dz-00 was detected, demonstrating the obvious enhancement effect was attributed to the proximate A provided by the complementary strand.

To further define the key role of adenine in EnEAA unambiguously, the effect of A•T base pairing was explored. As shown in Figure 2F, the formation of A•T base pair (Dz-62 a:b) totally blocks the EnEAA, and the activity of Dz-62 a:b is even lower than that of the original Dz-00. When this A is exposed with the removal of the T, the enhancement effect is restored (Dz-62a:c). Of special interest is that more mechanism knowledge of EnEAA on the molecular level can be obtained from this set of experiments. It is well-known that in A•T base pair through Watson–Crick hydrogen bonds, purine N1 and 6-amino group of adenine serve as the acceptor and donor of hydrogen bonds, respectively (Figure 2G). On this basis, it can be inferred that at least one of these two sites is involved in the catalysis process.

Peroxidative behavior of Dz-00 and Dz-11

Peroxidative behavior of Dz-00 and Dz-11 was studied in-depth aimed at further elucidating the functionality of terminal adenine. The catalytic cycle of G4 DNAzymes is generally believed to proceed through three steps (Figure 3A) (24,40): H_2O_2 readily binds to hemin (Fe(III)) and the following heterolytical O-O cleavage step leads to an intermediate (compound I) comprising a ferryl species (Fe(IV) = O) and a porphyrin cation radical, through a two-electron oxidation of hemin; compound I is then reduced to ferryl hemin (Fe(IV) = O) compound II and back to hemin (Fe(III)) via two sequential single-electron transfer reactions from substrate molecules ($ABTS^{2-}$). Detailed characterization of peroxidative behavior shows that the activities of both DNAzymes exhibit a zero-order dependence on $ABTS^{2-}$ concentration (Supplementary Figure S8), but display a linear kinetic behavior as a function of H_2O_2 concentration, revealing that the rate-determining step in the catalytic cycle is the hemin-activation step to form the compound I. The measured $V_{Dz\text{-}11}/V_{Dz\text{-}00}$ was a value of about 5 which was independent of H_2O_2 or $ABTS^{2-}$ concentration. To probe the possible compound I intermediate, we next investigated the effect of H_2O_2 addition on the electronic adsorption spectra of DNAzymes. Upon addition of H_2O_2, both DNAzymes displayed a hypochromicity of Soret band at 404 nm (Supplementary Figure S9). It is noticeable that the decay rate of Soret band of Dz-11 is remarkably faster than that of Dz-00 (Figure 3B). The absorption change of DNAzymes at visible region was also monitored for shedding more light on the intermediates of DNAzymes. Dz-11 showed the instant disappearance of E band (~500 nm) and D band (~630 nm) concomitant with the obvious increase in absorbance over 550–620 and 650–700 nm in 0.5 min after the reaction started (Figure 3C), indicating the generation of initial intermediate of G4–hemin complex (41). Sequentially, the overall decay over A450-700 nm occurred, evidencing the hemin degradation caused by successive re-

Table 1. Dissociation constants (K_d), catalytic activities (v, initial rates of DNAzyme-catalyzed peroxidation reaction) and absorption parameters of hemin, Dz-00-hemin and Dz-11-hemin complexes

	K_d	V	Soret		E band	D band	spin/coord
	(nM)	($\mu M \cdot min^{-1}$)	(nm)	ϵ_M	(nm)	(nm)	
hemin	/	0.4 ± 0.1	398	0.71×10^5			
Dz-00-hemin	36 ± 2	2.3 ± 0.3	404	1.48×10^5	501	628	HS/6C
Dz-11-hemin	30 ± 3	11.7 ± 0.6	404	1.46×10^5	501	629	HS/6C

Error represents the standard deviation of triplicate measurements.

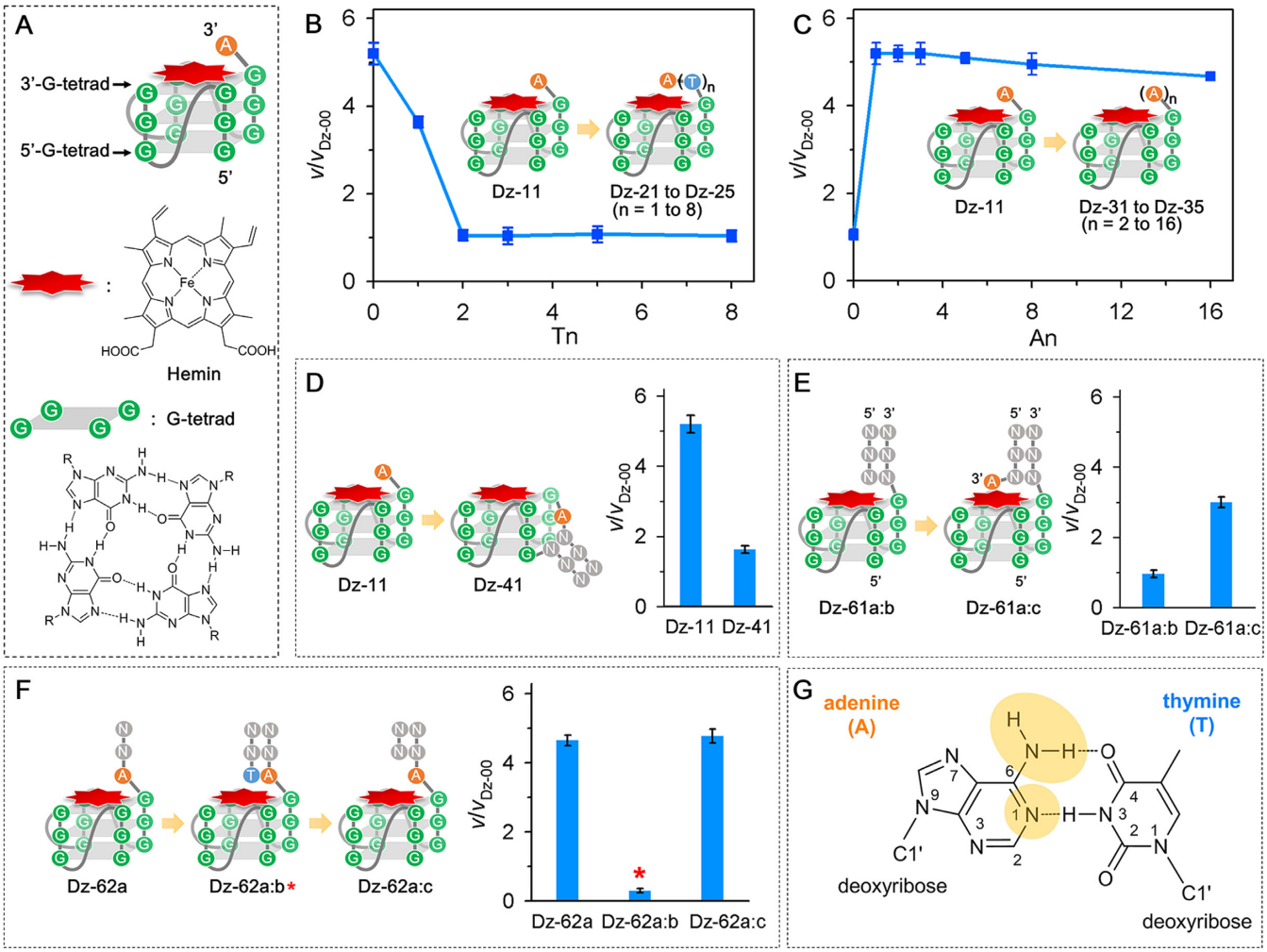

Figure 2. (**A**) Schematic structure of Dz-11-hemin complex (top), the chemical structures of hemin (middle) and G-tetrad (bottom). (**B**–**F**) The influences of different factors on EnEAA effect: (B) the different length of poly-T spacer between G4 core sequence and adenine base, (C) poly-A at 3′ terminal of G4 core sequence, (D) G4 structure with intramolecular duplex for restricting the orientation of adenine, (E) G4 structure with the proximate adenine nucleotide provided by the complementary strand and (F) the formation of A•T base pair. (G) The structure of A•T base pair. Error bar represents the standard deviation of triplicate measurements.

action with H_2O_2 (42). In contrast, in the case of Dz-00, the gradual diminishing of E and D bands as well as the slight increase of $A_{550\text{-}620\ nm}$ and $A_{650\text{-}700\ nm}$ were observed in the initial period of the reaction (0–2.5 min), implying a much slower formation of the initial intermediate of Dz-00 than Dz-11 (Figure 3C and D). Then similar overall decay of absorbance was determined. The absorption characteristics of the initially observed DNAzyme intermediate, such as decay of Soret band, diminish of E and D bands and increase in absorbance over A550-750 nm, resemble those of protein peroxidase compound I (43), in substantiation of the compound I-like intermediate. To sum up, our peroxidative behavior analysis has revealed that the EnEAA is achieved through the accelerated formation of the compound I.

The pH Dependence of Dz-11 and Dz-00 Activity

It is well-established that the ionizable histidine residue at distal position of protein peroxidases functions as the gen-

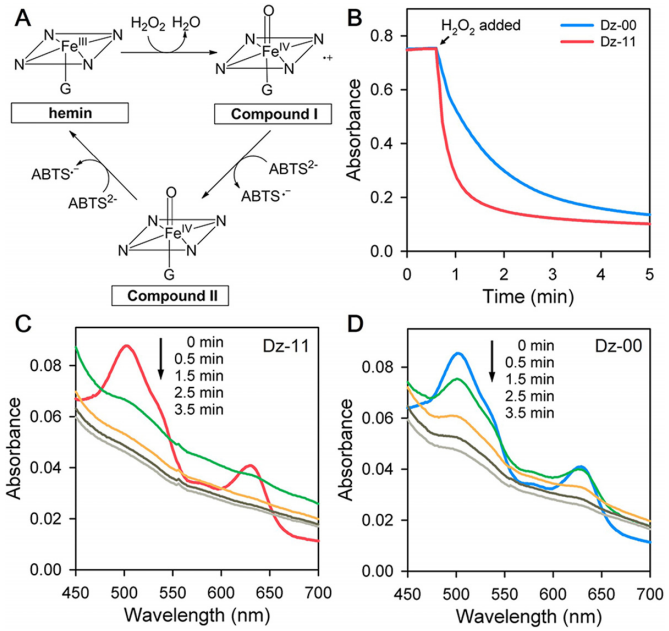

Figure 3. (**A**) Proposed peroxidation cycle facilitated by G-quadruplex DNAzyme for the $ABTS^{2-}$-H_2O_2 reaction. (**B**) Decay kinetics of the G4 DNAzymes' absorbance at 404 nm in the presence of H_2O_2 (2 mM). (**C** and **D**) Represent the time-dependent adsorption spectra change in visible region to probe the formation of compound I-like intermediate in the reaction process of the Dz-00-hemin (C) and Dz-11-hemin (D) with H_2O_2 (2 mM), respectively. The direction of absorbance change is indicated by the arrow.

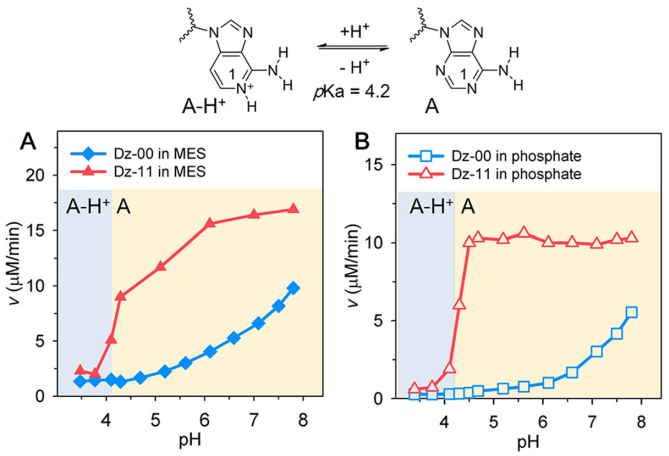

Figure 4. Plots of the initial peroxidation rates of Dz-00 (tetragonum) and Dz-11 (triangle) DNAzymes as a function of pH values in MES solution (**A**) and in phosphate solution (**B**).

eral acid–base catalyst to accelerate compound I formation as well as the overall peroxidation reaction, thus the rate profile of protein peroxidases shows a typical pH-dependent manner. This fact promoted us to evaluate the influence of pH on the catalytic efficiency of G4 DNAzymes. As shown in Figure 4A, the pH-rate profile of Dz-11 in MES buffer consists of two distinct ascending parts, evidencing that the deprotonation of two functional groups with apparent pK_a around pH 4.1 and pH 6.0, respectively, plays an important role for the activity. In comparison, Dz-00 displays different pH profile with only one ascending region with apparent pK_a in pH 6–7. To understand the dissimilarity, the pK_a values of adenine ($A\text{-}H^+/A$) and MES-Buffer, which are 4.2 (44) and 6.15 (45), respectively, are considered. Region with apparent pK_a in pH 6–7 can be attributed to the MES-buffer, a nitrogenous buffer, which has been demonstrated to facilitate peroxidation reactions via exogenous general acid–base catalysis (3,41). The marked difference of pH-rate profiles between two DNAzymes suggested that, besides the effect of nitrogenous buffer, the deprotonated adenine participates in the catalysis of peroxidation reaction and may even play a predominant role in pH 4–6. In order to eliminate the interference from the buffer effect, phosphate buffer was chosen because the oxyanion buffer affords relatively weak buffer effect (3). As shown in Figure 4B, the activity of Dz-11 sharply increases in the range of pH 4-4.5 and then reaches a plateau. The fact that the apparent pK_a near 4.3 is almost identical to the pK_a of adenine solidly supports the significance of the deprotonated adenine group as the endogenous active species in EnEAA. The steady activity of Dz-11 in a wide pH range from 5–8 indicates the key role of A-based catalysis and negligible influence of phosphate buffer. In contrast, the increase of the activity of Dz-00 is only observed when the pH is over 6, which is similar to the pH profile of G4 DNAzyme PS2.M in phosphate buffer (3). Furthermore, the pK_a values of Dz-11 and Dz-00 are calculated to be 8.78 and 8.74, respectively, from the spectrophotometric titration curves of resting DNAzymes (Supplementary Figure S10), close to that of PS2.M (8.7) (46). These results reveal that the high-spin aquo complex, the active form of resting DNAzyme, is the predominant species throughout the examined pH range (3–8), indicating that the pH-dependent activity difference between Dz-11 and Dz-00 is unrelated to the acid–base transition state of resting DNAzymes. Therefore, the pH-rate profiles clearly proved that the intrinsic activity of G4 DNAzyme could be switched by the ionization state of N1 of 3′A, providing another important hint on the mechanistic evaluation of EnEAA.

The molecular modeling of Dz-11 and Dz-00

The analysis of the micro-environment in the axial position of hemin, which is known to play crucial roles in accelerating compound I formation in natural and artificial peroxidases, is hereby necessary. Since crystal or NMR structure of G4 DNAzyme remains unexplored, we performed molecular docking and dynamics simulation by using AutoDock and NAMD programs to understand the hemin-binding micro-environment of G4 DNAzymes (47–49). As shown in Figure 5, hemin stacks well upon the 3′-G-quartet of Dz-00 and Dz-11. The hemin iron is situated close to the N3 atom of G3 in Dz-11 with a distance of 3 Å, whereas the iron is positioned 3.4 Å from the N1 atom of G8 in Dz-00. This calculation is consistent with the currently known knowledge that one of guanines constitutive of the G-quartet acts similarly to the proximal histidine ligand in natural enzyme HRP and forms a direct proximal coordination bond with iron center to stabilize the high-valence intermediates (35). Notably, the lack of nucleotide constitutive on the distal site of the hemin (away from 3′-G-quartets) in Dz-00 clearly

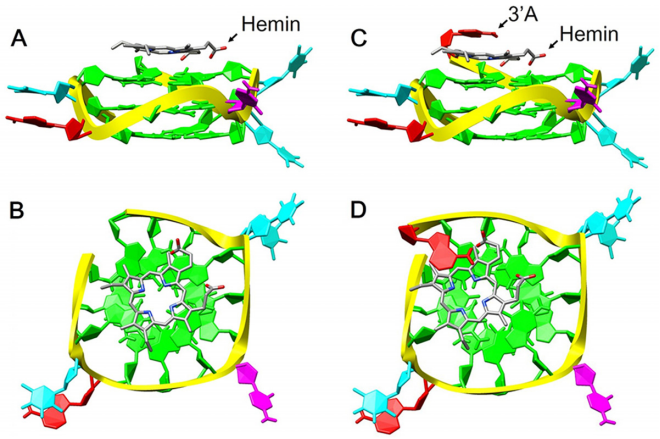

Figure 5. Molecular models of Dz-00-hemin (**A** and **B**) and Dz-11-hemin (**C** and **D**) complexes, respectively. A, C: side view, B and D: top view. Molecular docking studies were performed by AutoDock and the docking structures were prepared by Chimera 1.10.2.

supports that the prototype G4 DNAzyme lacks such a distal ligand analogous to distal histidine residue in HRP. In contrast, in Dz-11, the 3′A is positioned upon the distal side of the hemin and the heme group is slightly shifted toward the terminal adenine group, implying the possibility of 3′A as the distal ligand.

The mechanism analysis of EnEAA

Although several possible mechanisms could account for EnEAA, our observations supported that EnEAA occurred due to general acid–base catalysis: the linear reaction curves for all G4 DNAzymes (Figure 1) indicates that the auto-oxidation and degradation of both G4 sequences and hemin are negligible. Thus, it can be concluded that EnEAA doesn't arise from the extra protection by 3′A against the oxidative degradation of hemin or G4 sequence. This conclusion is further supported by the following evidences: (i) although guanine is more vulnerable to oxidation than adenine due to its lower reduction potential compared to adenine (50,51), 3′G shows no activity-enhancing effect (Figure 1); (ii) the variants with poly-A tail with increased local concentration of A, which are reasonably expected to provide more potent protection ability, can't further increase the activity (Figure 2C). (ii) Another possible mechanism is that additional adenine could provide extra π–π stacking or hydrophobic interaction with hemin, leading to better DNAzyme activity. However, it is challenged by the cases with 3′G or A•T base pair, in which similar or stronger π–π stacking is present but show no enhancement of the activity (Figure 2F). (iii) Since the purine N1 and 6-amino of adenine have been reported as metal ion binding sites (52), it is possible that 3′A replaces one of G in the G-quartet to act as the proximal ligand of hemin via direct coordinate-bonding. Nevertheless, this possibility can be precluded as additional adenine doesn't influence the adsorption spectroscopic features and the binding affinity of hemin with G-quadruplex (Table 1). (iv) Considering that the added A•T base pair totally eliminates EnEAA, the more plausible possibility is that adenine might form hydrogen bonds with the intermediates in the peroxidation process through its purine N1 and 6-amino groups. Besides, the pH-rate profile of the Dz-11 has proven the activity switch caused by the ionization of N1 of adenine and thus indicates that the adenine may act as general acid–base catalyst to accelerate the formation of compound I in G4-mediated peroxidation reaction.

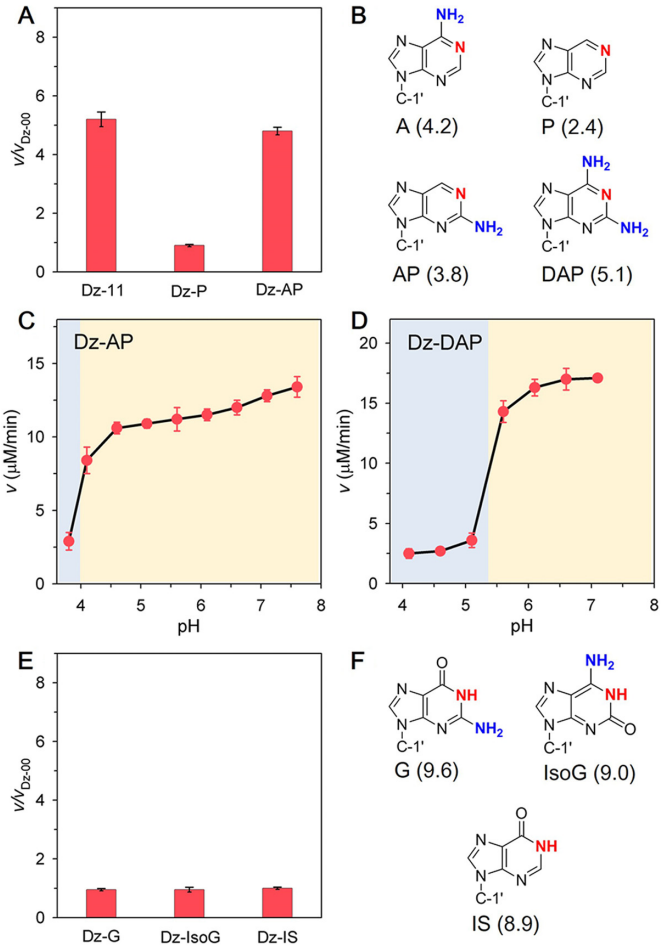

Figure 6. (**A** and **E**) The catalytic activities of DNAzymes with various purine derivatives at 3′ terminal of Dz-00 in pH 5.1. (**B** and **F**) The structures of purine derivatives. Their relative pK_a values are shown in brackets. (**C** and **D**) Plots of the initial peroxidation rates of AP (C) and DAP (D) modified DNAzymes as a function of pH values in MES solution. Error bar represents the standard deviation of triplicate measurements.

The activity of Dz-11 variants with 3′ nucleotide substitutions

To evaluate the functional groups of adenine responsible for the catalysis, we examined the effect of other purine analogs on the G4 DNAzyme activity, including three adenine analogs (purine (P), 2-Aminopurine (AP) and 2,6-Diaminopurine (DAP)) and two guanine analogs (isoguanine (IsoG) and inosine (IS)). When these purine analogs were used as 3′ end residue of DNAzymes (Figure 6A and B), the effect of AP (Dz-AP) on the peroxidation activity is very similar to A (Dz-11), but P (Dz-P) shows no effect on the DNAzyme activity, indicating the importance of an exocyclic amino group at the ortho-position of purine N1. Further pH dependence studies revealed that the pH-rate

profile of Dz-P was almost identical to that of Dz-00 (Supplementary Figure S11A), while all Dz-11, Dz-AP and Dz-DAP were similar in activity improvement and pH-rate profile (Figures 4A, 6C and D), except a slight difference on apparent pK_a of activity-ascending region, which is about 4.1, 4.0 and 5.4 for Dz-11, Dz-AP and Dz-DAP, respectively. Interestingly, these values perfectly match the pK_a values of N1 of A (4.2), AP (3.8) and DAP (5.1), suggesting the unprotonated N-1 of these purine analogs is significant for catalysis. As shown in Figure 6E and Supplementary Figure S11, all G derivatives (G, IsoG and IS) are unable to enhance the DNAzyme activity and exhibit the same pH-rate profile as Dz-00. These results are due to their N1 imino proton with pK_a about 9, thus they could not serve as proton acceptor in the first step of general base catalysis to receive a proton from hydrogen peroxide in the observed pH range (pH 3–8). Likewise, thymine is incapable of promoting catalysis because of its N3 imino proton. Although cytosine is similar to adenine in both the pK_a (4.6) and the structure (with unprotonated pyrimidine N3 and 4-amino group), 3′C led to only 1.5-fold increase of activity which is much weaker than 3′A (Figure 1). It probably results from that the amidine and amino groups of cytosine could orient in the same way as those of adenine, but they would be further from the H_2O_2-bound hemin center because of the smaller size of pyrimidine ring. Hence, all these results validated that both the unprotonated form of N1 of adenine and the vicinal exocyclic amino group were essential for DNAzymes to promote the peroxidation reaction.

For better understanding the roles of N1 and ortho-amino group in the catalysis, the interaction between adenine derivatives and H_2O_2 molecule were investigated by the quantum mechanical calculation. The calculations were carried out using DFT (B3LYP) and MP2 method with a basis set of aug-cc-pVDZ. The calculation results (Figure 7) show that the vicinal amino group and N1 group concertedly form two hydrogen bonds (N1—H—Oα and 6-NH—H—Oβ) with H_2O_2, causing multiply synergistic effects: (i) a pair of hydrogen bonds significantly enhances the interactions between adenine derivatives and H_2O_2, which is reflected by the increased binding energy (9.2, 9.0 and 9.0 kcal/mol for A, AP and DAP, respectively, versus 6.5 kcal/mol for P); (ii) In comparison with P/H_2O_2 complex, the shortened hydrogen bond of N1—H—Oα (1.781, 1.781 and 1.753 Å for A, AP and DAP, respectively, versus 1.830 Å for P) and the stretching vibration red-shift of H—Oα bond (3155, 3199 and 3109 cm^{-1} for A, AP and DAP, respectively, versus 3332 cm^{-1} for P) were observed in the other three complexes (A/H_2O_2, AP/H_2O_2 and DAP/H_2O_2). These data indicate that the synergy of hydrogen bonds strengthens the hydrogen bond between purine N1 and H_2O_2 but weakens the covalent bond H—Oα simultaneously, facilitating the proton transfer to N1 in the first step of general acid–base catalysis for the heterolytic cleavage of O-O bond.

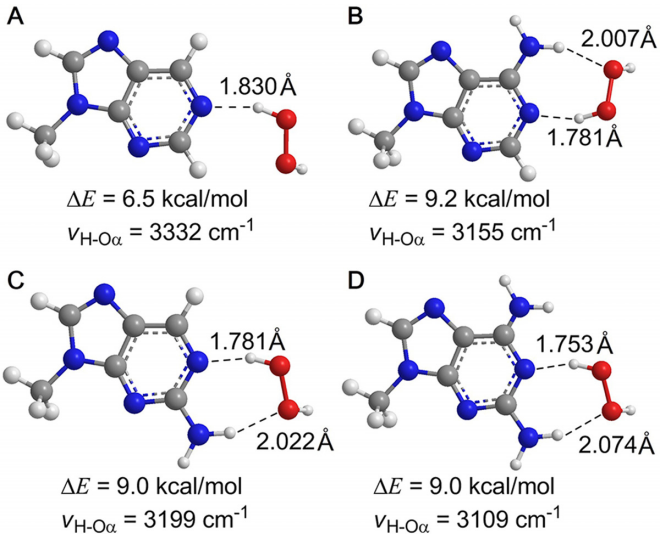

Figure 7. Optimized structures of purine derivatives with H_2O_2 at B3LYP/aug-cc-pVDZ and MP2/aug-cc-pVDZ level, where DE is the binding energy of the complex binding with H_2O_2 and $v_{H\text{-}O\alpha}$ is the H–Oα (in N1–H–Oα) stretching vibration of H_2O_2. (**A**): purine (P); (**B**): adenine (6-aminopurine, A), (**C**): 2-aminopurine (AP) and (**D**): 2,6-diaminopurine (DAP).

Potential mechanism of adenine-mediated G4 DNAzyme activity enhancement

Based on the information we gathered from above experiments, along with the well established catalytic mechanism of HRP, a potential mechanism for elucidating EnEAA is hereby proposed. As illustrated in Scheme 1, the resting G4 DNAzyme has a H_2O molecule coordinated with ferric center of hemin as distal ligand. The first step (step I) starts from the binding of H_2O_2 to the hemin to replace H_2O, with the concomitant donation of a proton to the N1 of adenine (proton receptor, as a base catalyst) from the α–oxygen atom bound to the heme iron (step II). Adjacent 6-amino group of adenine as a proton donor provides an H-bond to β–oxygen atom. Then, the proton transfers from the α–oxygen to N1 of adenine, leading to the deprotonation of H_2O_2 and the formation of a ferric-peroxide (Fe-OOH) complex (step III). Subsequently, the ionized adenine as acid catalyst gives the proton to the β–oxygen atom of the Fe–OOH complex along with the heterolytic cleavage of O-O bond (step IV). This catalytic cascade produces the compound I of DNAzyme. Collectively, the significance of the 3′A for EnEAA can be interpreted by the above supposition that N1 site of adenine promotes the formation of compound I by acting as a general acid–base catalyst, and the 6-amino group of adenine not only facilitates the binding of H_2O_2 to DNAzyme, but also contributes to stabilizing the transition state for compound I formation by interacting with the β–oxygen atom. Since the compound I generation is the rate-limiting step in the peroxidase catalytic circle, adenine accelerates the overall G4-DNAzyme catalytic circle via promoting compound I formation

The generality of EnEAA

We then addressed whether the EnEAA is a general strategy for improving the G4 DNAzyme activity. First, the substrate generality was examined by using AR, TMB and luminol as the substrates for fluorescent, UV-vis and chemiluminescent measurement, respectively. As shown in Supplementary Figure S12, for all the substrates tested, Dz-

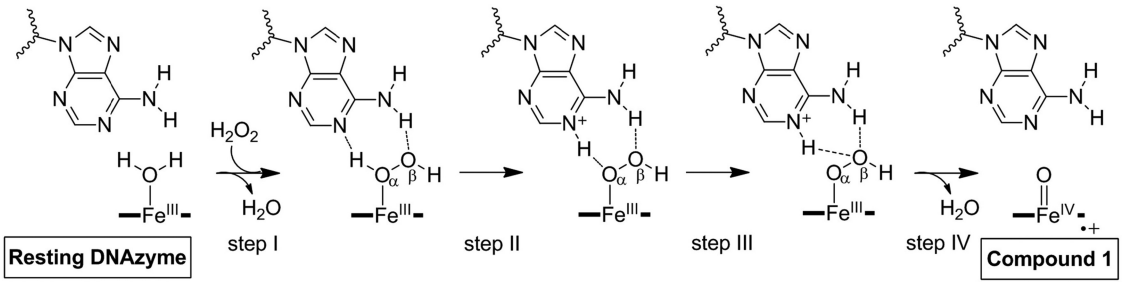

Scheme 1. The proposed mechanism of adenine-mediated acceleration of G4 peroxidase catalysis.

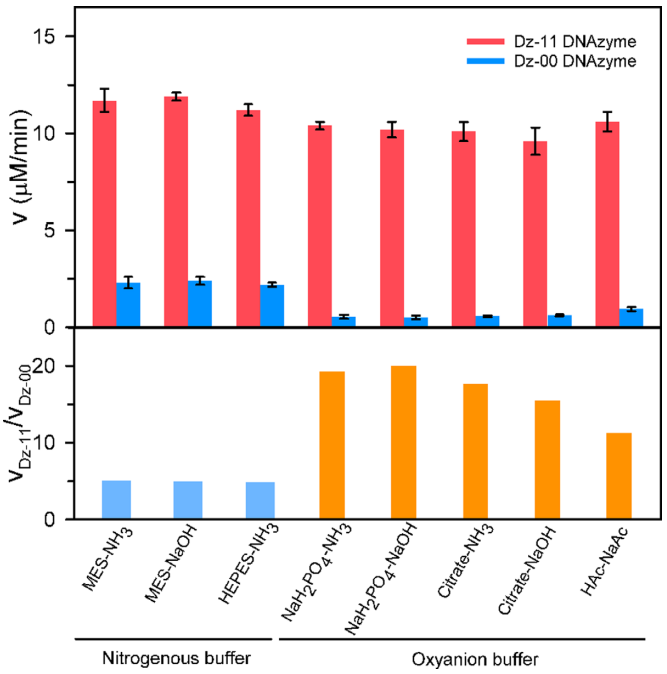

Figure 8. Catalytic rates (upper) and ratio (v_{Dz-11}/v_{Dz-00}, below) of Dz-00 and Dz-11 with different buffer species. [DNA] = 100 nM, [hemin] = 100 nM, [buffer] = 25 mM at pH 5.1. Error bar represents the standard deviation of triplicate measurements.

11 showed better catalytic activity (>2.5-fold) than Dz-00, proving the generality of the EnEAA for diverse substrates. Then, the activity of Dz-11 and Dz-00 in different buffers (25 mM, pH 5.1) was investigated. As shown in Figure 8, in general, the activity of Dz-00 shows a stronger dependence on buffer ingredient. Nitrogenous buffers appear to be more preferable to the peroxidation of Dz-00 than oxyanion buffers, which is consistent with previously reported results of PS2.M (3). It results from that Dz-00 lacks its distal ligand and, instead, exogenous nitrogenous species participate in catalyzing peroxidation. However, the activity of Dz-11 is almost unchanged in all the buffers examined, indicating that the adenine as an intramolecular catalytic residue can screen the buffer effect. Accordingly, due to the buffer-dependent Dz-00 activity, V_{Dz-11}/V_{Dz-00} is around 5-fold in nitrogenous buffers and significantly increases to above 10-fold in oxyanion buffers. Notably, the maximum of 20.0-fold was observed in phosphate buffer. These results demonstrate that the EnEAA is generally applicable for various buffers.

To assess the influence of G4 DNAzyme topological conformation on the EnEAA, several G4 sequences (19) (Supplementary Table S2) were utilized for comparison. Before the activity measurement, the conformation of all G4 were characterized by CD (Supplementary Figure S13). As shown in Table 2, all the DNAzymes with parallel structures show obvious EnEAA, whereas no enhancing effect is observed in any antiparallel G4 DNAzymes. We ascribe this unique topological preference to the fact that the diagonal loop of anti-parallel G-quadruplex are located on the top of the G-tetrad floor (53), which would impede the binding of hemin with G-tetrad and the interaction between hemin and the terminal A. Hence, it suggests that the EnEAA is generally efficient for the parallel G4 DNAzymes, implying the potential for rational modification of known parallel G4 DNAzymes for activity improvement. Moreover, these results can explain the high catalytic activity of some G4-DNAzymes, for example EAD2 (CTGGGAGGGAGGGAGGGA) which has the highest peroxidase activity in previous reports (19,21). It is a parallel G4 with an intrinsic 3′A, and the deletion of its 3′A leads to 3.4-fold decrease of DNAzyme activity, proving that its potent activity dependent on EnEAA.

To test whether the generality of EnEAA can be extended to G4 RNAzymes, experiments using RNA versions of Dz-00 and Dz-11, rDZ-00 and rDz-11 were carried out. As shown in Supplementary Figure S14, rDz-00 shows identical catalytic activity as Dz-00. Notably, rDz-11 with 3′A exhibits substantially enhanced peroxidative activity relative to rDz-00. V_{rDz-11}/V_{rDz-00} is ∼4.3 in MES buffer and 7.6 in phosphate buffer, clearly demonstrating the potency of EnEAA on G4 RNAzyme.

DISCUSSION

The discovery of EnEAA proves that a single adenine base can serve as the endogenous species to boost the peroxidation activity of G4 DNAzyme/RNAzyme. Compared to previously reported exogenous activity-boosting species, adenine as intramolecular boosting agents possesses several obvious advantages: (i) to afford the equivalent activity enhancement, the required concentration of 3′A (here is 100 nM, the same as the DNAzyme's concentration) is at least four order of magnitude lower than that of exogenous boosting agents (generally above 1 mM), owing to the intramolecular proximity effect of the adenine for the increase

Table 2. Peroxidase activities of different G-quadruplex structures including parallel and antiparallel structures with or without an adenine nucleotide at its 3′ terminal

Name	Structure	−3′ A	+3′ A	Ratio
c-Myc	parallel	2.7 ± 0.2	4.7 ± 0.1	1.7
EAD2	parallel	4.5 ± 0.1	15.3 ± 0.3	3.4
VEGF	parallel	2.0 ± 0.1	9.3 ± 0.4	4.7
HIF-1a	parallel	7.3 ± 0.6	13.7 ± 0.3	1.9
EAD4	parallel	2.1 ± 0.1	7.5 ± 0.1	3.6
Thrombin aptamer	antiparallel	0.9 ± 0.1	0.9 ± 0.1	1.0
G2T4	antiparallel	1.2 ± 0.1	1.3 ± 0.1	1.0
Oxy28	antiparallel	1.2 ± 0.1	1.2 ± 0.1	1.0

All the G-quadruplex structures were confirmed by CD (Supplementary Figure S14). [DNA] = 100 nM, [hemin] = 100 nM. Error represents the standard deviation of triplicate measurements.

of the effective concentration; (ii) the application of EnEAA is much more convenient and economical due to without the requirement of exogenous species; and (iii) the boosting effect of intramolecular A is remarkably less susceptible to the interference of environmental factors compared to exogenous reagents. It is also worth-mentioning that, in this original approach, we demonstrate the employment of just one single base is adequate to enhance the activity substantially (5–20 fold increase), differing from the reported activity-improving strategy by flanking d(CCC) sequence (∼3-fold increase) (29). More importantly, this unique EnEAA puts the endogenous DNA sequence capable of activity-boosting to the limit (single base).

Benefiting from the simplicity of the system with only single-base alternation, our data revealed that several conventional activity-enhancing mechanisms have been excluded, such as the alternation of G4 structure, stability or hemin binding affinity, protection against oxidative degradation, and the increment of hydrophobicity or π–π stacking, while adenine serving as a general acid–base species is the plausible mechanism accounting for EnEAA. Although adenine has been found to catalyze the hydrolysis of phosphodiester bond in hairpin ribozymes and Varkud satellite ribozymes (54–57), our findings give the first example of the catalytic function of the adenine in a distinct reaction category, peroxidation reaction. Moreover, it is of interest to note that adenine functions as the general acid–base species in G4 DNAzyme/RNAzyme similar to the distal histidine in natural HRP, which may lead us to promote the hypothesis that adenine is a likely prebiotic analog of histidine in the peroxidation catalysis in 'RNA world' hypothesis.

Based on the molecular modeling result and the catalytic function of adenine, we deduce that adenine is a potential distal ligand in G4–hemin complex. It is intriguing and suggestive because G4 DNAzyme/RNAzyme is conventionally believed to lack the intrinsic distal species. Thus, the findings will promote researches in the distal micro-environment of nucleic acid peroxidases which remain largely unknown. Admittedly, the improved activity of G4 DNAzyme by EnEAA is still moderate compared to that of protein peroxidases. It is probably decided by the fact that the potential distal site of G4 DNAzyme with only an adenine residue is remarkably primitive in structure and functionality compared to the complex distal pockets of the evolved protein counterparts which contains several well located catalytic residues. It is expected that several strategies can be adopted to further improve G4 DNAzyme activity via optimizing their distal environments: (i) screening a variety of modified bases and other organic molecules to select more potent distal catalytic species than adenine; (ii) increasing the range of functional residues by incorporating various catalytic building blocks, such as basic/acid, nucleophilic or hydrophobic groups; and (iii) building complex distal micro-environment through the arrangement of multiple distal species by different locating approaches.

Furthermore, the conventional method to obtain new G4 DNAzymes is *in vitro* selection (SELEX), which relies on optimizing the binding affinity of DNA sequence with hemin or other porphyrin derivatives (3,21). Since EnEAA is unrelated to hemin-binding affinity and applicable to various parallel G4 DNAzymes, and thus can be used as a 'post-selection' modification strategy to further promote the DNAzyme activity. In addition, as several new functions of G4 DNAzymes have been recently discovered (58,59), such as the enzymatic activity mimicking NADH oxidase and NADH peroxidase (59), the work to explore whether the EnEAA is able to improve these activities of G4–hemin complex is underway.

CONCLUSIONS

In summary, we reported a unique activity-enhancing mechanism (EnEAA) of G4 peroxidases mediated by an adjacent adenine nucleotide. We have demonstrated that the additional 3′A dramatically enhances G4 DNAzymes activity via accelerating the formation of compound I, and the functional groups of the adenine are ionizable N1 and exocyclic othro-amino group. Our results suggest that adenine may function as the distal species to perform general acid–base catalysis in G4 DNAzymes, providing a deep insight into the catalytic mechanism of peroxidase-mimicking G4 DNAzyme/RNAzyme. The catalytic role of adenine is similar to that of histidine in HRP, implying the possibility of adenine as a probiotic analog of histidine to catalyze peroxidation in 'RNA world' hypothesis. Moreover, the discovery of EnEAA will not only guide the improvement of known G4 DNAzymes by 'post-selection' modification, but also stimulate the rational design of advanced G4 DNAzymes via introducing specific catalytic species in distal site. These new findings have wide-ranging implications on various research fields ranging from nucleic acid biocatalyst to biomolecular diagnostics.

SUPPLEMENTARY DATA

Supplementary Data are available at NAR Online.

ACKNOWLEDGEMENT

We are grateful for helpful discussions with Prof Juewen Liu at the University of Waterloo in Canada, Dr Lirui Guan and Prof Honghui Wang at Hunan University.

FUNDING

National Natural Science Foundation of China [21575038, 21235002, 21305037]; Foundation for Innovative Research Groups of NSFC [21521063]; Young Top-notch Talent for Ten Thousand Talent Program; Natural Science Foundation of Hunan Province [2015JJ1005]; Fundamental Research Funds for the Central Universities.
Conflict of interest statement. None declared.

REFERENCES

1. Xu,Y. (2011) Chemistry in human telomere biology: structure, function and targeting of telomere DNA/RNA. *Chem. Soc. Rev.*, **40**, 2719–2740.
2. Travascio,P., Bennet,A.J., Wang,D.Y. and Sen,D. (1999) A ribozyme and a catalytic DNA with peroxidase activity: active sites versus cofactor-binding sites. *Chem. Biol.*, **6**, 779–787.
3. Travascio,P., Li,Y. and Sen,D. (1998) DNA-enhanced peroxidase activity of a DNA aptamer-hemin complex. *Chem. Biol.*, **5**, 505–517.
4. Breaker,R.R. and Joyce,G.F. (2014) The expanding view of RNA and DNA function. *Chem. Biol.*, **21**, 1059–1065.
5. Gilbert,W. (1986) Origin of life: the RNA world. *Nature*, **319**, 618.
6. Wang,F., Lu,C.H. and Willner,I. (2014) From cascaded catalytic nucleic acids to enzyme-DNA nanostructures: controlling reactivity, sensing, logic operations, and assembly of complex structures. *Chem. Rev.*, **114**, 2881–2941.
7. Willner,I., Shlyahovsky,B., Zayats,M. and Willner,B. (2008) DNAzymes for sensing, nanobiotechnology and logic gate applications. *Chem. Soc. Rev.*, **37**, 1153–1165.
8. Mao,X., Simon,A.J., Pei,H., Shi,J., Li,J., Huang,Q., Plaxco,K.W. and Fan,C. (2016) Activity modulation and allosteric control of a scaffolded DNAzyme using a dynamic DNA nanostructure. *Chem. Sci.*, **7**, 1200–1204.
9. Lu,C.H., Willner,B. and Willner,I. (2013) DNA nanotechnology: from sensing and DNA machines to drug-delivery systems. *ACS Nano*, **7**, 8320–8332.
10. Ihara,T., Ohura,H., Shirahama,C., Furuzono,T., Shimada,H., Matsuura,H. and Kitamura,Y. (2015) Metal ion-directed dynamic splicing of DNA through global conformational change by intramolecular complexation. *Nat. Commun.*, **6**, 6640.
11. Li,T., Lohmann,F. and Famulok,M. (2014) Interlocked DNA nanostructures controlled by a reversible logic circuit. *Nat. Commun.*, **5**, 4940.
12. Freeman,R., Liu,X. and Willner,I. (2011) Chemiluminescent and chemiluminescence resonance energy transfer (CRET) detection of DNA, metal ions, and aptamer-substrate complexes using hemin/G-quadruplexes and CdSe/ZnS quantum dots. *J. Am. Chem. Soc.*, **133**, 11597–11604.
13. Liu,Z., Li,W., Nie,Z., Peng,F., Huang,Y. and Yao,S. (2014) Randomly arrayed G-quadruplexes for label-free and real-time assay of enzyme activity. *Chem. Commun.*, **50**, 6875–6878.
14. He,K., Li,W., Nie,Z., Huang,Y., Liu,Z., Nie,L. and Yao,S. (2012) Enzyme-regulated activation of DNAzyme: a novel strategy for a label-free colorimetric DNA ligase assay and ligase-based biosensing. *Chem. Eur. J.*, **18**, 3992–3999.
15. Li,W., Liu,Z., Lin,H., Nie,Z., Chen,J., Xu,X. and Yao,S. (2010) Label-free colorimetric assay for methyltransferase activity based on a novel methylation-responsive DNAzyme strategy. *Anal. Chem.*, **82**, 1935–1941.
16. Wang,Z.G., Zhan,P. and Ding,B. (2013) Self-assembled catalytic DNA nanostructures for synthesis of para-directed polyaniline. *ACS Nano*, **7**, 1591–1598.
17. Pelossof,G., Tel-Vered,R., Elbaz,J. and Willner,I. (2010) Amplified biosensing using the horseradish peroxidase-mimicking DNAzyme as an electrocatalyst. *Anal. Chem.*, **82**, 4396–4402.
18. Abe,H., Abe,N., Shibata,A., Ito,K., Tanaka,Y., Ito,M., Saneyoshi,H., Shuto,S. and Ito,Y. (2012) Structure formation and catalytic activity of DNA dissolved in organic solvents. *Angew. Chem. Int. Ed.*, **51**, 6475–6479.
19. Cheng,X., Liu,X., Bing,T., Cao,Z. and Shangguan,D. (2009) General peroxidase activity of G-quadruplex−hemin complexes and its application in ligand screening. *Biochemistry*, **48**, 7817–7823.
20. Grigg,J.C., Shumayrikh,N. and Sen,D. (2014) G-quadruplex structures formed by expanded hexanucleotide repeat RNA and DNA from the neurodegenerative disease-linked C9orf72 gene efficiently sequester and activate heme. *PLoS One*, **9**, e106449.
21. Zhu,L., Li,C., Zhu,Z., Liu,D., Zou,Y., Wang,C., Fu,H. and Yang,C.J. (2012) In vitro selection of highly efficient G-quadruplex-based DNAzymes. *Anal. Chem.*, **84**, 8383–8390.
22. Kong,D.M., Yang,W., Wu,J., Li,C.X. and Shen,H.X. (2010) Structure-function study of peroxidase-like G-quadruplex-hemin complexes. *Analyst*, **135**, 321–326.
23. Nakayama,S. and Sintim,H.O. (2009) Colorimetric split G-quadruplex probes for nucleic acid sensing: improving reconstituted DNAzyme's catalytic efficiency *via* probe remodeling. *J. Am. Chem. Soc.*, **131**, 10320–10333.
24. Stefan,L., Denat,F. and Monchaud,D. (2012) Insights into how nucleotide supplements enhance the peroxidase-mimicking DNAzyme activity of the G-quadruplex/hemin system. *Nucleic Acids Res.*, **40**, 8759–8772.
25. Kong,D.M., Xu,J. and Shen,H.X. (2010) Positive effects of ATP on G-quadruplex-hemin DNAzyme-mediated reactions. *Anal. Chem.*, **82**, 6148–6153.
26. Stefan,L., Denat,F. and Monchaud,D. (2011) Deciphering the DNAzyme activity of multimeric quadruplexes: insights into their actual role in the telomerase activity evaluation assay. *J. Am. Chem. Soc.*, **133**, 20405–20415.
27. Stefan,L., Guedin,A., Amrane,S., Smith,N., Denat,F., Mergny,J.L. and Monchaud,D. (2011) DOTASQ as a prototype of nature-inspired G-quadruplex ligand. *Chem. Commun.*, **47**, 4992–4994.
28. Qi,C., Zhang,N., Yan,J., Liu,X., Bing,T., Mei,H. and Shangguan,D. (2014) Activity enhancement of G-quadruplex/hemin DNAzyme by spermine. *RSC Adv.*, **4**, 1441–1448.
29. Chang,T., Gong,H., Ding,P., Liu,X., Li,W., Bing,T., Cao,Z. and Shangguan,D. (2016), Activity enhancement of G-quadruplex/hemin DNAzyme by flanking d(CCC). *Chem. Eur. J.*, **22**, 4015–4021.
30. Rodríguez-López,J.N., Lowe,D.J., Hernández-Ruiz,J., Hiner,A.N.P., García-Cánovas,F. and Thorneley,R.N.F. (2001) Mechanism of reaction of hydrogen peroxide with horseradish peroxidase: identification of intermediates in the catalytic cycle. *J. Am. Chem. Soc.*, **123**, 11838–11847.
31. Poulos,T.L. (2014) Heme enzyme structure and function. *Chem. Rev.*, **114**, 3919–3962.
32. Shumayrikh,N., Huang,Y.C. and Sen,D. (2015) Heme activation by DNA: isoguanine pentaplexes, but not quadruplexes, bind heme and enhance its oxidative activity. *Nucleic Acids Res.*, **43**, 4191–4201.
33. Sen,D. and Poon,L.C.H. (2011) RNA and DNA complexes with hemin Fe(III) heme are efficient peroxidases and peroxygenases: how do they do it and what does it mean? *Crit. Rev. Biochem. Mol. Biol.*, **46**, 478–492.
34. Ozgen,M., Reese,R.N., Tulio,A.Z., Scheerens,J.C. and Miller,A.R. (2006) Modified 2, 2-Azino-bis-3-ethylbenzothiazoline-6-sulfonic acid (ABTS) method to measure antioxidant capacity of selected small fruits and comparison to ferric reducing antioxidant power (FRAP) and 2, 2′-diphenyl-1-picrylhydrazyl (DPPH) methods. *J. Agric. Food Chem.*, **54**, 1151–1157.
35. Zhu,X., Gao,X., Liu,Q., Lin,Z., Qiu,B. and Chen,G. (2011) Pb^{2+}-introduced activation of horseradish peroxidase (HRP)-mimicking DNAzyme. *Chem. Commun.*, **47**, 7437–7439.
36. Nicoludis,J.M., Miller,S.T., Jeffrey,P.D., Barrett,S.P., Rablen,P.R., Lawton,T.J. and Yatsunyk,L.A. (2012) Optimized end-stacking provides specificity of N-methyl mesoporphyrin IX for human telomeric G-quadruplex DNA. *J. Am. Chem. Soc.*, **134**, 20446–20456.

37. Phan,A.T., Kuryavyi,V., Gaw,H.Y. and Patel,D.J. (2005) Small-molecule interaction with a five-guanine-tract G-quadruplex structure from the human MYC promoter. *Nat. Chem. Biol.*, **1**, 167–173.
38. Zhang,L., Zhu,J., Guo,S., Li,T., Li,J. and Wang,E. (2013) Photoinduced electron transfer of DNA/Ag nanoclusters modulated by G-quadruplex/hemin complex for the construction of versatile biosensors. *J. Am. Chem. Soc.*, **135**, 2403–2406.
39. Liao,D., Chen,J., Li,W., Zhang,Q., Wang,F., Li,Y. and Yu,C. (2013) Fluorescence turn-on detection of a protein using cytochrome c as a quencher. *Chem. Commun.*, **49**, 9458–9460.
40. Li,T., Dong,S. and Wang,E. (2009) G-quadruplex aptamers with peroxidase-Like DNAzyme functions: which Is the best and how does it work? *Chem. Asian J.*, **4**, 918–922.
41. Travascio,P., Witting,P.K., Mauk,A.G. and Sen,D. (2001) The peroxidase activity of a hemin−DNA oligonucleotide complex: free radical damage to specific guanine bases of the DNA. *J. Am. Chem. Soc.*, **123**, 1337–1348.
42. Yang,X., Fang,C., Mei,H., Chang,T., Cao,Z. and Shangguan,D. (2011) Characterization of G-quadruplex/hemin peroxidase: substrate specificity and inactivation kinetics. *Chem. Eur. J.*, **17**, 14475–14484.
43. Dolphin,D., Forman,A., Borg,D.C., Fajer,J. and Felton,R.H. (1971) Compounds I of catalase and horse radish peroxidase: π-cation radicals. *Proc. Natl. Acad. Sci. U.S.A.*, **68**, 614–618.
44. Evans,T.A. and Seddon,K.R. (1997) Hydrogen bonding in DNA-a return to the status quo. *Chem. Commun.*, 2023–2024.
45. Klausen,J., Troeber,S.P., Haderlein,S.B. and Schwarzenbach,R.P. (1995) Reduction of substituted nitrobenzenes by Fe(II) in aqueous mineral suspensions. *Environ. Sci. Technol.*, **29**, 2396–2404.
46. Travascio,P., Sen,D. and Bennet,A.J. (2006) DNA and RNA enzymes with peroxidase activity—an investigation into the mechanism of action. *Can. J. Chem. Eng.*, **84**, 613–619.
47. Tachiwana,H., Miya,Y., Shono,N., Ohzeki,J.I., Osakabe,A., Otake,K., Larionov,V., Earnshaw,W.C., Kimura,H., Masumoto,H. *et al.* (2013) Nap1 regulates proper CENP-B binding to nucleosomes. *Nucleic Acids Res.*, **41**, 2869–2880.
48. Sandineni,A., Lin,B., MacKerell,A.D. Jr and Cho,B.P. (2013) Structure and thermodynamic insights on acetylaminofluorene-modified deletion DNA duplexes as models for frameshift mutagenesis. *Chem. Res. Toxicol.*, **26**, 937–951.
49. Jain,V., Hilton,B., Lin,B., Jain,A., MacKerell,A.D. Jr, Zou,Y. and Cho,B.P. (2013) Structural and thermodynamic insight into escherichia coli uvrABC-mediated incision of cluster diacetylaminofluorene adducts on the NarI sequence. *Chem. Res. Toxicol.*, **26**, 1251–1262.
50. Steenken,S. and Jovanovic,S.V., (1997) How easily oxidizable is DNA? One-electron reduction potentials of adenosine and guanosine radicals in aqueous solution. *J. Am. Chem. Soc.*, **119**, 617–618.
51. Seidel,C.A.M., Schulz,A. and Sauer,M.H.M., (1996) Nucleobase-specific quenching of fluorescent dyes. 1. Nucleobase one-electron redox potentials and their correlation with static and dynamic quenching efficiencies. *J. Phys. Chem.*, **100**, 5541–5553.
52. Patel,D.K., Domínguez-Martín,A., Brandi-Blanco,M.P., Choquesillo-Lazarte,D., Nurchi,V.M. and Niclós-Gutiérrez,J. (2012) Metal ion binding modes of hypoxanthine and xanthine versus the versatile behaviour of adenine. *Coordin. Chem. Rev.* **256**, 193–211.
53. Nakayama,S., Wang,J. and Sintim,H.O. (2011) DNA-based peroxidation catalyst—what is the exact role of topology on catalysis and is there a special binding site for catalysis? *Chem. Eur. J.*, **17**, 5691–5698.
54. Liberman,J.A., Guo,M., Jenkins,J.L., Krucinska,J., Chen,Y., Carey,P.R. and Wedekind,J.E. (2012) A Transition-state interaction shifts nucleobase ionization toward neutrality to facilitate small ribozyme catalysis. *J. Am. Chem. Soc.*, **134**, 16933–16936.
55. Ditzler,M.A., Sponer,J. and Walter,N.G. (2009) Molecular dynamics suggest multifunctionality of an adenine imino group in acid-base catalysis of the hairpin ribozyme. *RNA*, **15**, 560–575.
56. Kuzmin,Y.I., Costa,C.P.D., Cottrell,J.W. and Fedor,M.J. (2005) Role of an active site adenine in hairpin ribozyme catalysis. *J. Mol. Biol.*, **349**, 989–1010.
57. Meli,M., Vergne,J. and Maurel,M.C. (2003) *In vitro* selection of adenine-dependent hairpin ribozymes. *J. Biol. Chem.*, **278**, 9835–9842.
58. Poon,L.C.H., Methot,S.P., Morabi-Pazooki,W., Pio,F., Bennet,A.J. and Sen,D. (2011) Guanine-rich RNAs and DNAs that bind heme robustly catalyze oxygen transfer reactions. *J. Am. Chem. Soc.*, **133**, 1877–1884.
59. Golub,E., Freeman,R. and Willner,I. (2011) A hemin/G-quadruplex acts as an NADH oxidase and NADH peroxidase mimicking DNAzyme. *Angew. Chem. Int. Ed.*, **50**, 11710–11714.